Article

Synthesis of Energetic 7-Nitro-3,5-dihydro-4*H*-pyrazolo [4,3-*d*][1,2,3]triazin-4-one Based on a Novel Hofmann-Type Rearrangement

Fu-Qiang Bi [1], Yi-Fen Luo [1], Jun-Lin Zhang [1,2,*], Huan Huo [1] and Bo-Zhou Wang [1,*]

[1] Xi'an Modern Chemistry Research Institute, Xi'an 710065, China; bifuqiang@msn.com (F.-Q.B.); luoyiluoyiluoyi204@163.com (Y.-F.L.); huohuan-234@163.com (H.H.)
[2] College of Chemistry & Materials Science, Northwest University, Xi'an 710127, China
* Correspondence: junlin-111@163.com (J.-L.Z.); wbz600@163.com (B.-Z.W.)

Abstract: Rearrangement reactions are efficient strategies in organic synthesis and contribute enormously to the development of energetic materials. Here, we report on the preparation of a fused energetic structure of 7-nitro-3,5-dihydro-4*H*-pyrazolo[4,3-*d*][1,2,3]triazin-4-one (NPTO) based on a novel Hofmann-type rearrangement. The 1,2,3-triazine unit was introduced into the fused bicyclic skeleton from a pyrazole unit for the first time. The new compound of NPTO was fully characterized using multinuclear NMR and IR spectroscopy, elemental analysis as well as X-ray diffraction studies. The thermal behaviors and detonation properties of NPTO were investigated through a differential scanning calorimetry (DSC-TG) approach and *EXPLO5* program-based calculations, respectively. The calculation results showed similar detonation performances between NPTO and the energetic materials of DNPP and ANPP, indicating that NPTO has a good application perspective in insensitive explosives and propellants.

Keywords: synthesis; NPTO; Hofmann-type rearrangement; mechanism; crystal

1. Introduction

As has been well-recognized, rearrangement reactions are the most efficient strategies in organic synthesis, which normally achieve the desired frameworks with remarkably high efficiency [1]. Meanwhile, rearrangement reactions are also important to the synthetic studies of energetic materials, especially for the formations of fused molecular skeletons or functional groups. For instance, an amino group (-NH$_2$) is a key structural unit for the formation of energetic groups such as nitro (-NO$_2$) and nitroamine (-NNO$_2$) groups. Moreover, the strong hydrogen bonding effect between -NH$_2$ and other O-rich groups normally plays an important role in achieving insensitivities and heat resistance properties of energetic materials [2,3]. Therefore, the introduction of -NH$_2$ groups is significant in the synthesis of energetic materials. A Curtius rearrangement is one of the most effective methods to convert the carbonyl structures connected to the energetic framework into amino structures, which has been applied to the synthesis of cage-like frameworks and nitrogen-rich aromatic ring energetic materials, such as octanitrocubane (ONC) and 4,4′-dinitro-3,3′-diazenofuroxan (DDF) [4–7]. (Figure 1)

Similar to a Curtius rearrangement, a Hofmann rearrangement is another widely applied reaction for the conversion of carbonyl structures to amino structures. For amide-based substrates, bromine (or chlorine) can be applied for the formation of amino structures under alkaline conditions. However, thus far, the applications of Hofmann reactions in the synthesis of energetic materials have rarely been reported, especially in the construction of new framework structures. Nitropyrazoles are significant for the design and synthesis of energetic materials [8,9]. During the past few decades, our research interest was mainly focused on the structural diversity of fused-heterocyclic frameworks in energetic

materials, among which, the pyrazolo [4,3-c]pyrazole structure was a successfully applied framework in the construction of 1*H*,4*H*-3,6-dinitropyrazolo [4,3-*c*]pyrazole (DNPP), as well as its insensitive derivative [10–13], 1,4-diamino-3,6-dinitropyrazolo[4,3-c]pyrazole (LLM-119) [14], which contains both amino and nitro groups. 1*H*,4*H*-3-Amino-6-nitropyrazolo[4,3-*c*]pyrazole (ANPP) is another pyrazolo[4,3-c]pyrazole framework-based insensitive energetic material that is ideal as the key intermediate for subsequent transformations in the design and synthesis of multiple kinds of pyrazole-based energetic materials [15–17]. Herein, we reported a brand-new Hofmann-type rearrangement that lead to a novel fused aromatic compound of 7-nitro-3,5-dihydro-4*H*-pyrazolo[4,3-*d*][1–3] triazin-4-one (NPTO) during our recent studies toward ANPP through a traditional Hofmann rearrangement. (Figure 2) The new compound of NPTO was fully characterized using multinuclear NMR and IR spectroscopy, elemental analysis as well as X-ray diffraction studies. Its thermal behaviors and detonation properties were investigated through a differential scanning calorimetry (DSC-TG) approach and *EXPLO 5* program-based calculations, respectively.
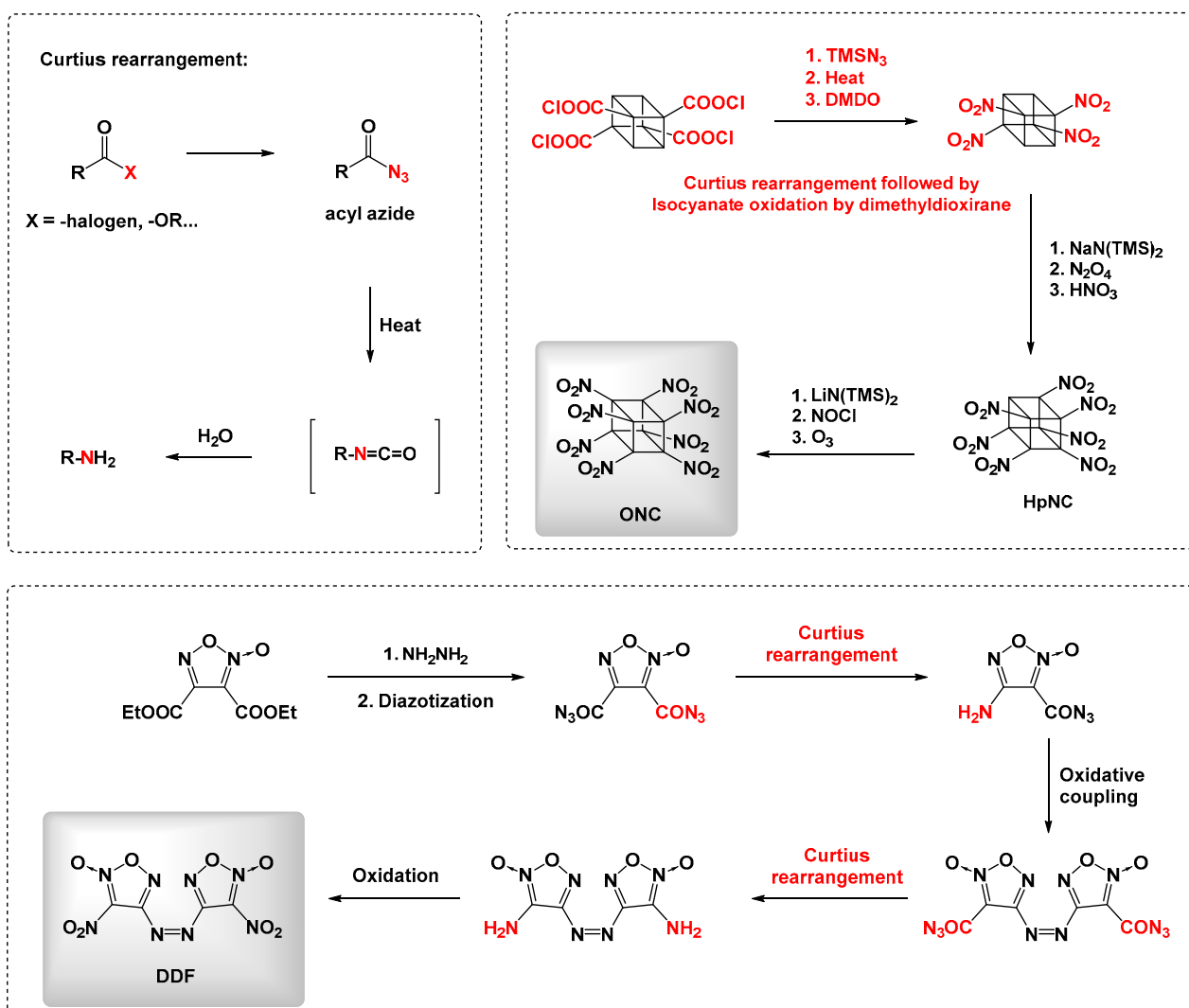

Figure 1. Curtius rearrangement in the synthesis of energetic materials.
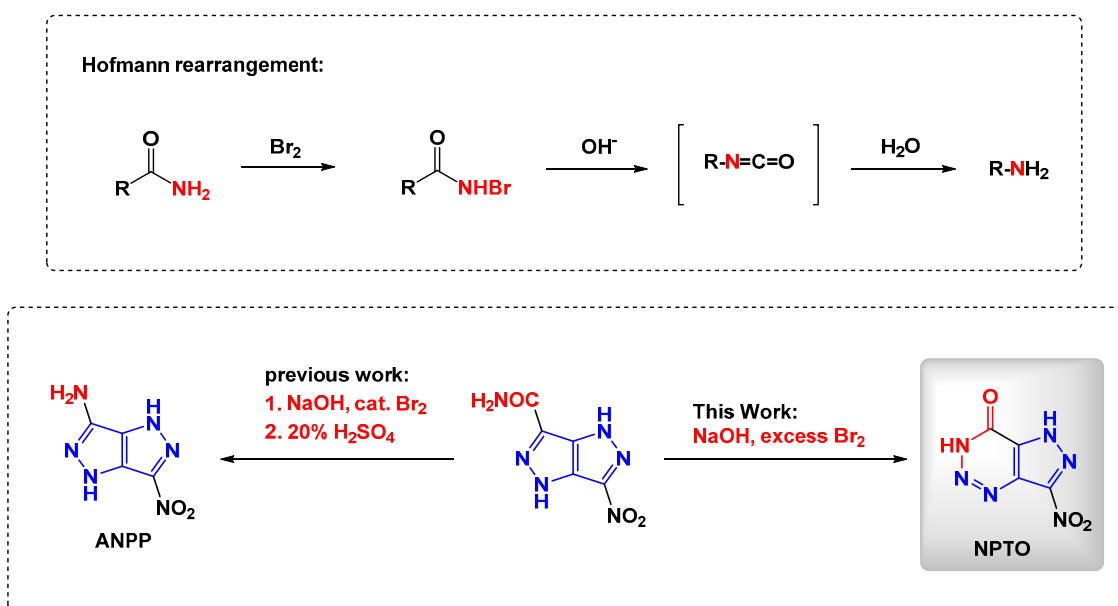
Figure 2. Hofmann rearrangement and the synthesis of NPTO.

2. Results and Discussion

2.1. Synthesis and Characterization towards NPTO

Starting from 1*H*,4*H*-3-carboxy-6-nitropyrazolo[4,3-*c*]pyrazole, the synthesis of ANPP was carried out through methyl esterification, amidation and a Hofmann rearrangement with the addition of a catalytic amount of Br$_2$ [18]. However, when we treated compound **1** with excess bromine in aqueous sodium hydroxide, an interesting Hofmann-type ring-expansion rearrangement was achieved, leading to the formation of NPTO with a yield of 45%. (Scheme 1, Figures S5 and S6)
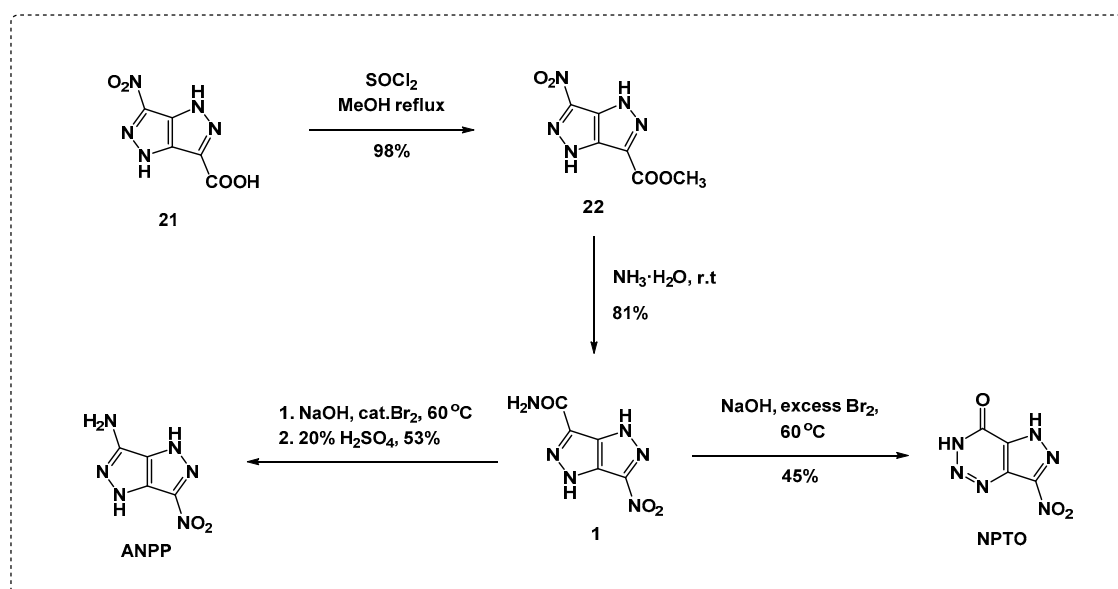
Scheme 1. Synthetic routes towards NPTO.

In order to explain the insensitive characteristics of NPTO from a structural point of view, NPTO was characterized through single crystal X-ray diffraction. (Figure S4) The crystal was obtained by dissolving NPTO in a mixture of ethanol/water, and detailed information on the crystallographic data is given in Table 1. The single-crystal X-ray diffraction results proved that the compound belongs to the monoclinic crystal system, space group $P2(1)/n$. Two molecules of water were wrapped in the crystal structure, leading to a low density of 1.693 g/cm^3. The entire molecule presented a planar structure, with the twist angles close to 0° or 180° (O2-N1-C1-N2 (0.779°), C1-C2-N6-N5 (−178.775°)). The length of the C1-N1 bond connected to the nitro group is 1.4453 (4) Å, which is obviously shorter than that of common carbon–nitrogen bonds, indicating a strong conjugated effect [19]. The molecular stacking diagram of the crystals is a standard "layer by layer" pattern with "π-π" stacking interactions and a layer spacing of 3.7254 Å [20]. As has been proved in the insensitive structures of TATB and LLM-105, strong hydrogen bonds can significantly reduce the "hot spots" in a crystal [21–24]. There are seven types of intermolecular hydrogen bonds (N4-H2 . . . N4″ (3.0100 Å, 143.2°), O4-H4B...O3 (2.8837(4)Å, 162.9°), N3-H1 . . . O5 (2.6453 Å, 170.0°), N4′-H2′ . . . N2 (3.0100 Å, 143.2°), O5′-H5A′ . . . O1 (2.9985 Å, 170.7°), O4-H4A′ . . . N6 (2.8907 Å, 165.1°) and O5-H5A...O4 (2.7407(7)Å, 178.2°)), which explained the excellent insensitive performances of NPTO [25,26]. (Figure 3).

Table 1. Crystallographic details of NPTO·2H$_2$O.

Compound	NPTO·2H$_2$O
Formula	C$_4$H$_6$N$_6$O$_5$
Formula weight	218.15
T (K)	296(2)
λ (Å)	0.71073
Crystal system	Monoclinic
Space group	$P2(1)/n$
a (Å)	6.608(3)
b (Å)	9.330(4)
c (Å)	13.998(6)
Volume (Å^3)	855.7(7)
Z	4
Dc (g/cm^3)	1.693
F (000)	448
θ range/(°)	2.63 to 25.09
Reflections collected/unique	4177/1519 [R$_{(int)}$ = 0.0623]
Refinement method	Full-matrix least-squares on F^2
GOF on F^2	1.002
Final R indexes (I > 2σ(I))	R$_1$ = 0.0560, wR$_2$ = 0.1254
Final R indexes (all data)	R$_1$ = 0.1058, wR$_2$ = 0.1498
Largest diff peak and hole (e Å^{-3})	0.322 and −0.222
GOF on F$_2$	0.949
CCDC number	2082280

2.2. Studies on Thermal Behaviors of NPTO

The thermal behaviors of the NPTO·2H$_2$O crystal were investigated based on the TG-DSC experiments. (Figures S1–S3) According to the experimental results, the thermal decomposition of the NPTO·2H$_2$O crystal can clearly be divided into two stages. The DSC analysis chart of NPTO is shown in Figure 1. It can be seen that NPTO has an endothermic peak in the temperature range of 52–84 °C, and the peak temperature is 68.47 °C. Combined with the structural characterization of the compound, this is the process of removing crystal water from the compound. After the loss of crystal water, the compound is relatively stable before reaching the decomposition temperature. The initial exothermic temperature of NPTO is 160.5 °C, and the exothermic peak temperature is around 179 °C. The exothermic peak of the thermal decomposition of NPTO is sharp, with a large heat release. The TG-

DTG analysis chart of NPTO is shown in Figure 4. It can be seen from the Figure 4 that the thermal decomposition of NPTO is divided into at least two stages. The previous process is the process of losing crystal water, with a total weight loss of 16.78%. The sample is stable before 164 °C, and the maximum weight loss peak appears at 178 °C. When the temperature reaches 180.5 °C, the cumulative decomposition depth of the sample is 95.62%. With a further rise in the heating temperature, the substance further decomposes and finally leaves 1.53% of black "residue".
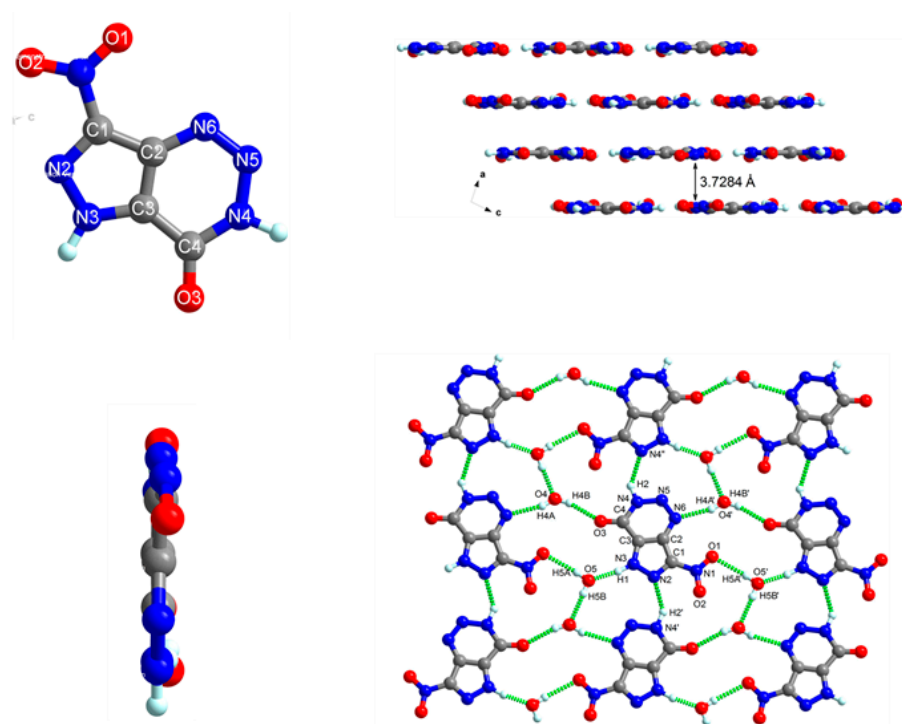

Figure 3. Molecular structure of NPTO·2H$_2$O and its crystal packing.
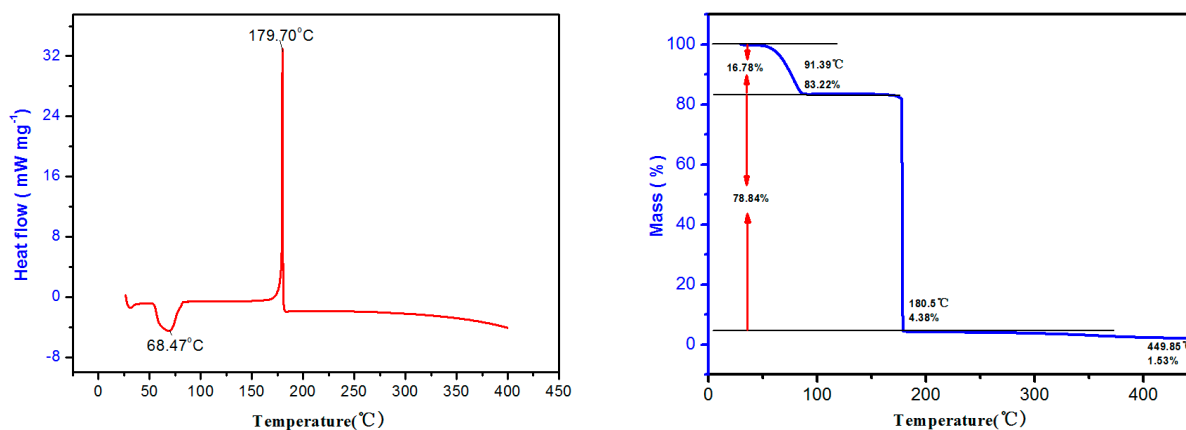

Figure 4. DSC-TG experiments of NPTO·2H$_2$O.

The thermodynamic parameters of the thermal decomposition process of NPTO will be useful when evaluating the safety properties of the compound. (Figure 5) The Kissinger method (Equation (1)) was applied for the calculation of the thermal decomposition activation energy (E_a) and the pre-exponential factor (A) of NPTO, where β_i is the heating rate and T_{pi} is the peak temperature at different heating rates [27]. In addition, according to T_{pi} and E_a at different heating rates, the initial thermal decomposition peak temperature T_{p0} (when the heating rate β approaches 0) can be obtained using Equation (2). When

the heating rate β approaches 0, the values of E, A and T will be E_a, A_a and T_{p0}. The activation enthalpy ($\Delta H^{\neq}$) can be calculated through Equations (3) and (4), where k_B is Boltzmann's constant and h is Plank's constant. All the results are shown in Table 2. The high E_a indicates a slow decomposition rate and potential long-term storage.

$$ln\left(\frac{\beta_i}{T_{Pi}^2}\right) = ln\left(\frac{A_aR}{E_a}\right) - \frac{E_a}{RT_{Pi}}$$ (1)

$$T_{Pi} = T_{P0} + a\beta_i + b\beta_i^2 + c\beta_i^3$$ (2)

$$A = \frac{k_BT}{h}exp\left(\frac{\Delta S^{\neq}}{R} + 1\right)$$ (3)
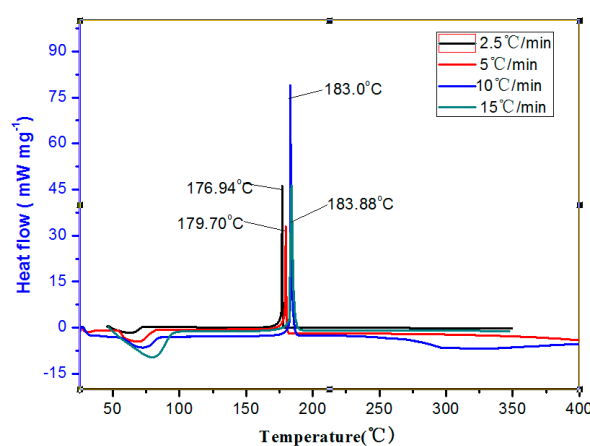
$$\Delta H^{\neq} = E - RT$$ (4)

Figure 5. DSC experiments of NPTO·2H$_2$O at different heating rates.

Table 2. Thermodynamic parameters of the thermal decomposition process of NPTO.

Heating Rates β/(°C/min)	T_{pi}/(°C)	E_a/(kJ·mol^{-1})	lg(A_a/s^{-1})	T_{p0}/ (°C)	$\Delta H^{\neq}$/ (KJ·mol^{-1})
2.5	176.94			173.33	427.70
5	179.7				
10	183.0	429.14	27.33		
15	183.88				

2.3. ESP Analysis Studies of NPTO

Electrostatic potential (ESP) is a real and fundamentally significant physical property of compounds as it provides information about charge density distribution and molecular reactivity [28–30]. Therefore, the surface electrostatic potential was taken into consideration in the analysis of the electronic properties of NPTO. The electrostatic potential of DNPP was calculated for comparison. The ESP-mapped surfaces of DNPP and NPTO are presented in Figure 6. Some pivotal maxima and minima of ESP are expressed by orange and cyan spheres, respectively. It can be seen from Figure 6 that the strongly positive ESPs distribute in the central regions of molecules and above C-NO$_2$ and N-H bonds, while the negative ones concentrate on the edges of molecules, especially on the oxygen atoms of nitro groups. It was proposed by Politzer et al. [31] that the impact sensitivity of explosives has a positive correlation with the surface potential maxima ($V_{s,max}$), namely, the impact sensitivity increases with a higher positive value of $V_{s,max}$. The global $V_{s,max}$ of NPTO (68.26 kcal/mol) is higher than that of DNPP (64.44 kcal/mol), indicating that the impact sensitivity of NPTO may be higher compared with DNPP. According to Zeman et al.,

the increase in negative surface potential minima ($V_{s,min}$) and/or the sum of $V_{s,max}$ and $V_{s,min}$ (V_{tot}) corresponds to an increase in the detonation velocity (D). The global V_{tot} of NPTO and DNPP are 34.03 and 39.39 kcal/mol, respectively. It is not hard to see that V_{tot} decreases as compared to DNPP. Accordingly, it can be speculated that NPTO possesses a lower detonation velocity than DNPP.
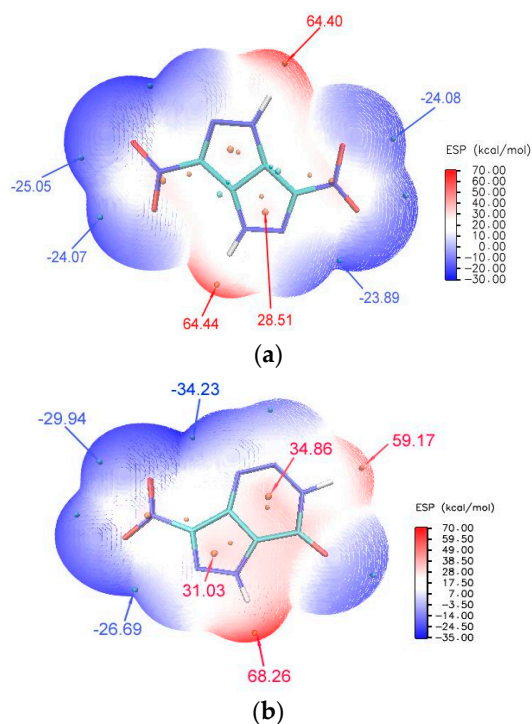

(**a**)

(**b**)

Figure 6. ESP-mapped surfaces of DNPP (**a**) and NPTO (**b**).

2.4. SEM Morphology of NPTO

The morphology of NPTO was examined with a HITACHI (Japan) S-3400N-II Scanning Electron Microscope (SEM) at 5 kV and 10 mA. (Figure S7) Crystal quality, including the crystal shape, surface and defects, plays an important role in the safe storage and transport of an energetic material, and ultimately affects the detonation performance of the explosive [32,33]. As shown in Figure 7, the crystal exhibits a colorless-prism-type morphology with a uniform size, regular structure and smooth surface. Considering the crystal's approximate spherical shape, which can increase the charge density to a great degree; it is a good candidate for practical application as an energetic material.
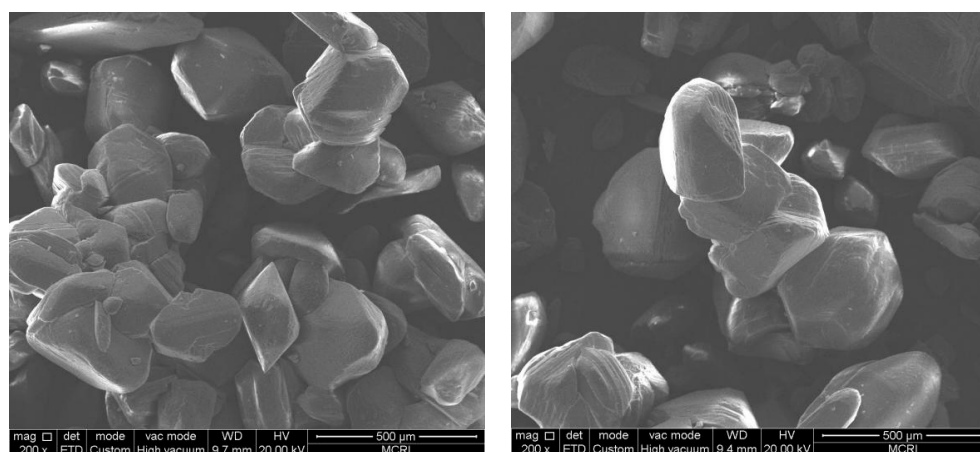

Figure 7. SEM Morphology graphs of NPTO.

2.5. Studies on Detonation Performances of NPTO

Studies on the detonation properties of the NPTO were carried out through quantum computations methods with the Gaussian 09 (Revision A. 02) suite of programs. [34] The optimized structures were characterized to be true local energy minima on the potential-energy surface without imaginary frequencies. The gas phase heats of formation were calculated with the atomization method using the Gaussian 09 program package at the b3lyp/6-311g** level of theory [34–36]. The gas phase heat of formation was transformed to solid phase heat of formation using Trouton's rule [37,38]. Based on the density and heat of formation calculated, the detonation properties for NPTO were calculated by EXPLO5 6.04 [39]. All the data are summarized in Table 3.

Table 3. Calculated physico-chemical properties and detonation parameters of NPTO.

Compound	ρ [a] $(g \cdot cm^{-3})$	ΔH_f [b] $(kj \cdot mol^{-1})$	D [c] $(m \cdot s^{-1})$	P [d] (Gpa)	H_{50} [e] (cm)	H_{50} [f] (J)
ANPP	1.678	283.28	7317	19.79	44.63	10.94
DNPP	1.758	290.44	8068	26.96	33.98	8.32
NPTO	1.752	217.13	7556	22.32	40.44	9.91

[a] Crystal density. [b] Molar enthalpy of formation. [c] Detonation velocity. [d] Detonation pressure. [e] Impact sensitivity.
[f] Friction sensitivity.

NPTO showed great insensitivities toward the impact and friction stimulations. From a structural point of view, the aromatic system size can significantly affect the characteristics of highly energetic compounds, especially their sensitivity toward detonation. This influence usually results in a decrease in the sensitivity of these compounds toward detonation. Typical examples include the insensitive explosives of 2,2′,4,4′,6,6′-hexanitrostilbene (HNS) and 2,2,4,4,6,6-hexanitroazobenzene (HNAB), whose conjugation between aromatic rings have been well known to increase stability in explosives. Obviously, the conjugation between aromatic rings of NPTO also played a similar role, leading to its excellent insensitivities toward external stimulations.

3. Conclusions

In this study, we achieved the synthesis of NPTO based on a unique Hofmann-type reaction. This synthetic strategy is the first time that a Hoffmann-type reaction has been used for the construction of a fused skeleton in the research field of energetic materials. Through NMR, elemental analysis, X-single crystal diffraction and other means, the structure of NPTO has been fully characterized. DSC-TG studies showed NPTO has good thermal stability. Further theoretical studies have further shown that the energy density level of NPTO is close to that of DNPP, while the sensitivity level is better than that of DNPP, making it an ideal candidate for the develop of insensitive explosives.

Institutional Review Board Statement: Not applicable.

Informed Consent Statement: Not applicable.

Data Availability Statement: Not applicable.

Conflicts of Interest: The authors declare no conflict of interest.

References

1. Surya, K.D. *Rearrangement Reactions in Applied Organic Chemistry: Reaction Mechanisms and Experimental Procedures in Medicinal Chemistry. II*; Wiley-VCH Verlag GmbH & Co. KGaA: Weinheim, Germany, 2021.
2. Zeman, S.; Marcela, J. Sensitivity and performance of energetic materials. *Propellants Explos. Pyrotech.* **2016**, *41*, 426–451. [CrossRef]
3. Zhang, C.Y. Origins of the energy and safety of energetic materials and of the energy & safety contradiction. *Propellants Explos. Pyrot.* **2018**, *43*, 855–856.
4. Zhou, J.; Zhang, J.L.; Ding, L.; Bi, F.Q.; Wang, B.Z. Progress in the Construction of Cage-like Skeleton Energetic Compounds. *Chin. J. Energ. Mater.* **2019**, *27*, 708–716.
5. Zhang, M.X.; Eaton, P.E.; Gilardi, R. Hepta and octanitrocubanes. *Angew. Chem. Int. Ed.* **2000**, *39*, 401–404. [CrossRef]
6. Binnikov, A.N.; Kulikov, A.S.; Mahkova, N.N.; Ochinnikov, O.V.; Pivina, T.S. 4-Amino-3-azidocarbonyl furoxan as a universal synthon for the synthesis of energetic compounds of the furoxan series. In Proceedings of the 30th International Annual Conference of ICT, Karlsrruhe, Germany, 29 June–2 July 1999; pp. 58/1–58/10.
7. Guo, T.; Liu, M.; Huang, X.C.; Wang, Z.J.; Qiu, S.J.; Ge, Z.X.; Meng, Z.H. Efficient preparation and comprehensive properties of thermal decomposition and detonation for 4,4′-dinitro-3,3′-azofuroxan. *J. Anal. Appl. Pyrolysis* **2017**, *128*, 451–458. [CrossRef]
8. Chen, D.X.; Xiong, H.L.; Yang, H.W.; Tang, J.; Cheng, G.B. Nitropyrazole based tricyclic nitrogen-rich cation salts: A new class of promising insensitive energetic materials. *FirePhysChem* **2021**, *1*, 71–75. [CrossRef]
9. Wu, B.; Yang, L.F.; Zhai, D.D.; Ma, C.M.; Pei, C.H. Facile synthesis of 4-amino-3,5-dinitropyrazolated energetic derivatives via 4-bromopyrazole and their performances. *FirePhysChem* **2021**, *1*, 76–82. [CrossRef]
10. Yin, P.; Zhang, J.H.; Mitchell, L.A.; Parrish, D.A.; Shreeve, J.M. 3,6-Dinitropyrazolo[4,3-c]pyrazole -Based Multipurpose Energetic Materials through Versatile N-Functionalization Strategies. *Angew. Chem. Int. Ed.* **2016**, *55*, 12895–12897. [CrossRef]
11. Li, Y.N.; Shu, Y.J.; Wang, B.Z.; Zhang, S.Y.; Zhai, L.J. Synthesis, structure and properties of neutral energetic materials based on N-functionalization of 3,6-dinitropyrazolo [4,3-c]pyrazole. *RSC Adv.* **2016**, *6*, 84760–84768. [CrossRef]
12. Dalinger, I.L.; Shkineva, T.K.; Vatsadze, I.A.; Popova, G.P.; Shevelev, S.A. N-Fluoro derivatives of nitrated pyrazole-containing fused heterocycles. *Mendeleev Commun.* **2011**, *21*, 48–49. [CrossRef]
13. Zhang, W.Q.; Xia, H.L.; Yu, R.J.; Zhang, J.H.; Wang, K.C.; Zhang, Q.H. Synthesis and properties of 3,6-Dinitropyrazolo-[4,3-c] Pyrazole(DNPP) Derivatives. *Propellants Explos. Pyrotech.* **2020**, *45*, 546–553. [CrossRef]
14. Li, Y.N.; Tang, T.; Lian, P.; Luo, Y.F.; Yang, W.; Wang, Y.B.; Li, H.; Zhang, Z.Z.; Wang, B.Z. Synthesis, thermal performance and quantum chemistry study on 1,4-diamino-3,5-dinitropyrazolo [4,3-c]pyrazole(LLM-119). *Chin. J. Org. Chem.* **2012**, *32*, 580–588. [CrossRef]
15. Piercey, D.G.; Chavez, D.E.; Scott, B.L.; Imler, G.H.; Parrish, D.A. An Energetic Triazolo-1,2,4- Triazine and its N-Oxide. *Angew. Chem. Int. Ed.* **2016**, *55*, 15315–15318. [CrossRef] [PubMed]
16. Schulze, M.C.; Scott, B.L.; Chavez, D.E. A high density pyrazolo-triazine explosive (PTX). *J. Mater. Chem. A* **2015**, *3*, 17963–17965. [CrossRef]
17. Tang, Y.X.; He, C.L.; Imler, G.H.; Parrish, D.A.; Shreeve, J.M. Aminonitro Groups Surrounding a Fused Pyrazolo-triazine Ring: A Superior Thermally Stable and Insensitive Energetic Material. *ACS Appl. Energy Mater.* **2019**, *2*, 2263–2267. [CrossRef]
18. Shevelev, S.A.; Dalimger, I.L.; Shkineva, T.K.; Ugrak, B.I.; Gulevskaya, V.I.; Kanishchev, M.I. Nitropyrazoles 1. Synthesis, transformations, and physicochemical properties of nitro derivatives of 1H,4H-pyrazolo[4,3-c]pyrazole. *Russ. Chem. Bull.* **1993**, *42*, 1063–1068. [CrossRef]
19. Allen, F.H.; Kennard, O.; Watson, D.G.; Brammer, L.; Orpen, A.G.; Taylor, R. Tables of bond lengths determined by X-ray and neutron diffraction. Part 1. Bond lengths in organic compounds. *J. Chem. Soc. Perkin Trans. 2* **1987**, *12*, S1–S19. [CrossRef]
20. Zhang, C.Y.; Wang, X.C.; Huang, H. π–stacked interactions in explosive crystals: Buffers against external mechanical stimuli. *J. Am. Chem. Soc.* **2008**, *130*, 8359–8365. [CrossRef]
21. Boddu, V.M.; Viswanath, D.S.; Ghosh, T.K.; Damavarapu, R. 2,4,6-Triamino-1,3,5-trinitrobenzene (TATB) and TATB-based Formulations−A Review. *J. Hazard. Mater.* **2010**, *181*, 1–8. [CrossRef]
22. Kretić, D.S.; Radovanovića, J.I.; Veljković, D.Ž. Can the sensitivity of energetic materials be tuned by using hydrogen bonds? Another look at the role of hydrogen bonding in the design of high energetic compounds. *Phys. Chem. Chem. Phys.* **2021**, *23*, 7472–7479. [CrossRef]
23. Zhou, J.; Zhang, J.L.; Wang, B.Z.; Qiu, L.L.; Xu, R.Q.; Sheremetev, A.B. Recent Synthetic Efforts towards High Energy Density Materials: How to Design High-Performance Energetic Structures? *FirePhysChem* **2021**, in press. [CrossRef]
24. Hu, L.; Staples, R.J.; Shreeve, J.M. Hydrogen bond system generated by nitroamino rearrangement: New character for designing next generation energetic materials. *Chem. Commun.* **2021**, *57*, 603–606. [CrossRef] [PubMed]
25. Yin, P.; Mitchell, L.A.; Parrish, D.A.; Shreeve, J.M. Energetic N-Nitramino/N-Oxyl-Functionalized Pyrazoles with Versatile π–π Stacking: Structure–Property Relationships of High-Performance Energetic Materials. *Angew. Chem. Int. Ed.* **2016**, *55*, 14409. [CrossRef]

26. Xue, Q.; Bi, F.Q.; Zhang, J.L.; Wang, Z.J.; Zhai, L.J.; Huo, H.; Wang, B.Z.; Zhang, S.Y. A Family of Energetic Materials Based on 1,2,4-Oxadiazole and 1,2,5-Oxadiazole Backbones with Low Insensitivity and Good Detonation Performance. *Front. Chem.* **2020**, *7*, 942–951. [CrossRef]

27. Kissinger, H.E. Reaction kinetics in differential thermal analysis. *Anal. Chem.* **1957**, *29*, 1702–1706. [CrossRef]

28. Wu, C.L.; Cheng, H.J.; Gou, R.J.; Jia, H.Y.; Zhang, S.H. Molecular Dynamics Study on Intermolecular interaction of CL-20/MDNI Composite Explosive. *Chin. J. Explos. Propellants* **2017**, *40*, 66–72.

29. Xie, Z.B.; Hu, S.Q.; Cao, X. Theoretical insight into the influence of molecular ratio on the binding energy and mechanical property of HMX/2-picoline-N-oxide cocrystal, cooperativity effect and surface electrostatic potential. *Mol. Phys.* **2016**, *114*, 2164–2176. [CrossRef]

30. Yuan, S.; Gou, B.W.; Guo, S.F.; Xiao, L.; Hu, Y.B.; Chen, T.; Hao, G.Z.; Jiang, W. reparation, Characterization and Properties of A New CL-20/TKX-50 Cocrystal Explosive. *Chin. J. Explos. Propellants* **2020**, *43*, 167–172.

31. Politzer, P.; Murray, J.S. The fundamental nature and role of the electrostatic potential in atoms and molecules. *Theor. Chem. Acc.* **2002**, *108*, 134–142. [CrossRef]

32. Hou, C.H.; Zhang, Y.P.; Chen, Y.G.; Jia, X.L.; Zhang, S.M.; Tan, Y.X. Fabrication of Ultra-Fine TATB/HMX Cocrystal Using a Compound Solvent. *Propellants Explos. Pyrotech.* **2018**, *43*, 916–922. [CrossRef]

33. Liu, K.; Zhang, G.; Luan, J.Y.; Chen, Z.Q.; Su, P.F.; Shu, Y.J. Crystal structure, spectrum character and explosive property of a new cocrystal CL-20/DNT. *J. Mol. Struct.* **2016**, *1110*, 91–96. [CrossRef]

34. Frisch, M.J.; Trucks, G.W.; Schlegel, H.B.; Scuseria, G.E.; Robb, M.A.; Cheeseman, J.R.; Montgomery, J.A., Jr.; Reven, T.V.; Kudin, K.N.; Burant, J.C.; et al. *Gaussian~09 {R}evision {E}.01*; Gaussian, Inc.: Wallingford, CT, USA, 2009.

35. Montgomery, J.A.; Frisch, M.J.; Ochterski, J.W.; Petersson, G.A. A complete basis set model chemistry. VII. Use of the minimum population localization method. *J. Chem. Phys.* **2000**, *112*, 6532–6542. [CrossRef]

36. Ochterski, J.W.; Petersson, G.A.; Montgomery, J.A. A complete basis set model chemistry. V. Extensions to six or more heavy atoms. *J. Chem. Phys.* **1996**, *104*, 2598–2619. [CrossRef]

37. Westwell, M.S.; Searle, M.S.; Wales, D.J.; Williams, D.H. Empirical correlations between thermodynamic properties and inter-molecular forces. *J. Am. Chem. Soc.* **1995**, *117*, 5013–5015. [CrossRef]

38. Zhang, Y.Q.; Parrish, D.A.; Shreeve, J.M. Derivatives of 5-nitro-1,2,3-2H-triazole-high performance energetic materials. *J. Mater. Chem. A* **2013**, *1*, 585–593. [CrossRef]

39. Suceska, M. EXPLO5, Version 6.04. 2017. Available online: https://www.ozm.cz/explosives-performance-tests/thermochemical-computer-code-explo5/ (accessed on 28 November 2021).